



Shahrood University of  
Technology



Iranian Society of  
Mining Engineering  
(IRSM)

## Evaluation of Pressure-Settlement Response of Square Footing Rested on Sand Reinforced with Coir Geotextile

Jitendra Singh Yadav<sup>1</sup>, Poonam Shekhawat<sup>2\*</sup>, and Sreekeshava K S<sup>2</sup>

1- Department of Civil Engineering, NIT Kurukshetra, India

2- Department of Civil Engineering, Jyothy Institute of Technology, Bangalore, India

### Article Info

Received 13 October 2023

Received in Revised form 7  
December 2023

Accepted 21 December 2023

Published online 21 December  
2023

DOI: [10.22044/jme.2023.13721.2539](https://doi.org/10.22044/jme.2023.13721.2539)

### Keywords

Coir geotextile

Ultimate bearing capacity

Sand

Numerical modelling

### Abstract

The present work aims to assess the pressure-settlement behaviour of sand beds under a square footing reinforced with coir geotextile using the PLAXIS 3D software. The angle of internal friction of sand was varied from 28° to 38°. The effect of length of coir geotextile (1B, 2B, 3B, 4B, and 5B; B is width of footing) and position of coir geotextile (0.2B, 0.4B, 0.6B, 0.8B, and 1B) to ultimate bearing capacity of sand were examined. A remarkable improvement in ultimate bearing capacity of sand beds was obtained with provision of coir geotextiles. It was observed that the bearing capacity of sand increases by placing coir geotextiles up to a depth of 0.4B from base of footing, thereafter it starts decreasing. The optimum length of coir geotextile was found as 4B-5B. An insignificant improvement in the bearing capacity ratio of sand reinforced with coir geotextile was observed at higher values of angle of internal friction.

### 1. Introduction

Soil is an extremely complicated, heterogeneous, and erratic substance that has been exposed to the whims of weather with no control. It is usually considered as a mixture of four essential constituents: clay, silt, sand, and gravel. Usually, it has low shear and tensile strength [1]. The ultimate bearing capacity of the soil can be determined by various theories as suggested by Terzaghi (1943), Meyerhof (1951), Hansen's (1961) and Vesic's (1973) [2-5].

The Terzaghi bearing capacity equation for soils is given by:

$$Q_{ult} = c' N_c + q N_q + 0.5 \gamma B N_\gamma \quad (1)$$

Where:

$Q_{ult}$  = Ultimate bearing capacity of soil (pressure at which the soil fails)

$c'$  = Effective cohesion of the soil,

$q$  = Overburden pressure or effective vertical stress at foundation base,

$\gamma$  = Unit weight of soil,

$B$  = Width or diameter of the foundation in feet or meters,

$N_c, N_q, N_\gamma$  = Bearing capacity factors related to the soil type, calculated based on the angle of internal friction ( $\phi$ ) and the shape and depth of the foundation.

Terzaghi (1943) [2] assumed the failure zones was not to extend above the base level of footing. Thus, the shearing resistance of soil surrounding it above its base level was neglected. The proposed method was valid only  $D_f \leq B$  only. These limitations were overcome by Meyerhof (1951) [3].

$$Q_{ult} = c' N_c s_c d_c i_c + q N_q s_q d_q i_q + 0.5 \gamma B N_\gamma s_\gamma d_\gamma i_\gamma \quad (2)$$

where:

$s_c, s_q, s_\gamma; d_c, d_q, d_\gamma;$  and  $i_c, i_q, i_\gamma$  stand for shape factor, depth factor, and inclination factor. For cohesive soil, Hansen's bearing capacity theory (1961) [4] gave better correlation than the Terzaghi equation.

The soil reinforcement is a method to enhance the engineering behavior of soil, viz. shear strength, hydraulic conductivity, density, and compressibility. The method of soil reinforcement has achieved admiration in the construction of geotechnical infrastructure such as embankments, retaining walls, foundation, and pavements, due to the flexibility, versatility, and eco-friendly nature [6–10]. Thus the main objective of reinforcing soil substance is to enhance its bearing capacity, stability, and reduce the settlement and lateral deformation.

One of the main issues in foundation engineering is the proposing a cost-effective footing and secure transfer of load to the foundation soil [11–15]. There are numerous methods by means of which the bearing capacity of the foundation soil can be improved. Coir is a sustainable fiber that is extensively used to oppress the erosion trouble [16]. When knitted into geotextiles and positioned on areas which require erosion restriction, it advocates new vegetation by soaking up the moisture and averting topsoil from becoming dry. Coir geotextiles have a natural capability to hold moisture and shield the sun's radiation similar to natural soil, and unlike geosynthetic materials, it delivers good soil reinforcement allowing natural vegetation to become established. One of the uses of geotextiles is under the foundation. The coir geotextile plays a vital role in conserving nature. Because of the long-lasting characteristics, it delivers better functioning compared to other natural geotextiles [17–22].

Previously, numerous researchers have methodically tested the effectual application of several configurations of coir with the aim of soil reinforcement to enhance the engineering behaviour of soil [23–29]. Rao et al. [30] studied the influence of coir fibres and coir geotextile on the mechanical behaviour of sand and concluded that both fibres and geotextile enhanced the performance of sand specimen. The study further suggested the application of coir geotextile in rural roads and for ground improvement. Sayida et al. [31] observed less distress in coir geotextile reinforced paved road, after conducting cyclic load test on a lab model, compared to unreinforced road. Additionally, change in characteristic deflection, dynamic cone penetration indices, and about 50% improvement in field California bearing ratio

values were achieved for the coir geotextile reinforced paved road. Lal et al. [32] detected significant increase in strength and improvement in settlement properties with the inclusion of coir geotextile reinforced sand bed. Improvement in bearing capacity by a factor of 2.57 and settlement reduction by 73% was achieved by introduction of even a single layer of coir geotextile. Lal et al. [33] observed better settlement properties of a sand bed reinforced with coir geocell compared to the planar forms. The maximum increment in bearing capacity for coir geocell was observed as 7.92 compared to 5.83 in the case of planar forms for a settlement of 15% of foundation width. Lal et al. [34], in another study, examined behaviour of sand reinforced with coir geotextile in various forms through a series of triaxial compression tests. Strength enhancement and stiffness behaviour was observed for reinforcement sand. Vinod and Bhaskar [35] studied the behaviour of woven coir geotextile reinforced sand under a model square footing. The study suggested that the potential utilization of woven coir geotextile in subsoil had improved the strength by three times with the use of even a single layer of geotextile. Subaida et al. [36] investigated the tensile and interface characteristics of woven coir geotextile through an experimental programme. It was observed that the bond resistance of coir geotextile-sand interface is higher than shear strength of soil at low normal stress.

From the studies reported so far, it would appear that despite the potential of coir products as a reinforcement material, they have been under-utilized. A detailed study addressing the effect of length of coir geotextile, and position of coir geotextile on the ultimate bearing capacity of soil is required. This paper reports a detailed numerical study on the pressure-settlement behaviour of sand beds under a square footing reinforced with coir geotextile using the PLAXIS 3D software. The angle of internal friction of sand was varied from 28° to 38°. The effect of length of coir geotextile (1B, 2B, 3B, 4B, and 5B; B is width of footing) and position of coir geotextile (0.2B, 0.4B, 0.6B, 0.8B, and 1B) to ultimate bearing capacity of sand were examined.

## 2. Finite Element Modeling

### 2.1 Problem definition and model parameters

Numerical analysis is one of the tremendous mathematical implements which assist in resolving complex engineering glitches [37–46]. In this research work, a three-dimensional numerical

investigation was conducted to analyze the performance of sand reinforced with coir geotextile. The numerical analysis model used in the present study had dimensions of 2.4 m along the x-axis, 2.4 m along the y-axis, and 3.0 m along the z-axis. The water table was kept at 3.0 m. The

dimensions of the square footing used were 2.0 m × 2.0 m, and the thickness was kept at 0.5 m. A schematic illustration of the model and model developed in Plaxis 3D is shown in Figures 1 (a) and (b), respectively.

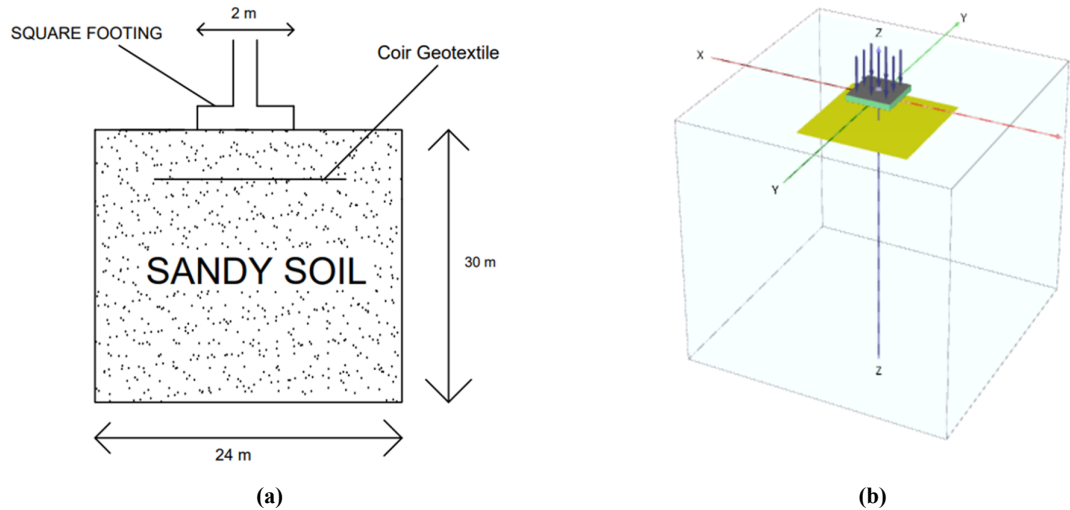


Figure 1. (a) Schematic diagram of the problem (b) Model developed in PLAXIS 3D.

The modeling in PLAXIS 3D was conducted in basically five steps including soil, structure, mesh, flow conditions, and staged construction. In the first step, the dimension of the model and the type of soil have been defined using the materials options. Four types of sandy soils were used in the analysis, and their properties are shown in Table 1. The Mohr-Coulomb model was used for each of the soil. The footing surface was made of concrete with the aim to replicate the weaker flexible interface (default interface strength factor = 1), indicating that the interface is not strong enough regarding the

adjacent soil (PLAXIS 3D foundation material models manual, version 1.5). The value of cohesion was kept at 0.3 kPa. The poisson ratio of 0.3 was used for all the types of sand. The footing and coir parameters used are tabulated in Tables 2 and 3, respectively. The length of coir geotextile was varied from 1B to 5B in step of 1B. The position of coir geotextile was varied as 0.2B, 0.4B, 0.6B, 0.8B, and 1B from the base of footing. The angles of internal friction of sand were taken as 28°, 30°, 34°, and 38°.

Table 1. Properties of soil sample.

Angle of internal friction ( $\phi$ )	Unit weight of soil $\gamma$ (kN/m <sup>3</sup> )	Model	Poisson's ratio (assumed)	Young's modulus (E) of soil (MPa)	Angle of dilatancy ( $\psi = \phi - 30^\circ$ )
28°	13.0	Mohr-Coulomb	0.30	18	0
30°	14.0	Mohr-Coulomb	0.30	24	0
34°	16.0	Mohr-Coulomb	0.30	30	4
38°	18.0	Mohr-Coulomb	0.30	48	8

Table 2. Footing parameters.

Dimension of footing	Unit weight (kN/m <sup>3</sup> )	Model	Young's modulus (GPa)	Poisson's ratio
2 x 2 m	24	Linear Elastic	20	0.15

Table 3. Coir geotextile parameters.

Identification	Material Type	Axial Stiffness (kNm)
Coir Geotextile	Elastic	1000

### 3. Results and Discussion

The obtained pressure-settlement behaviours of sand beds under a square footing reinforced with

coir geotextile are shown in Figures 2 to 5. The position and length of coir geotextile and type of soil on the bearing capacity are discussed in this section.

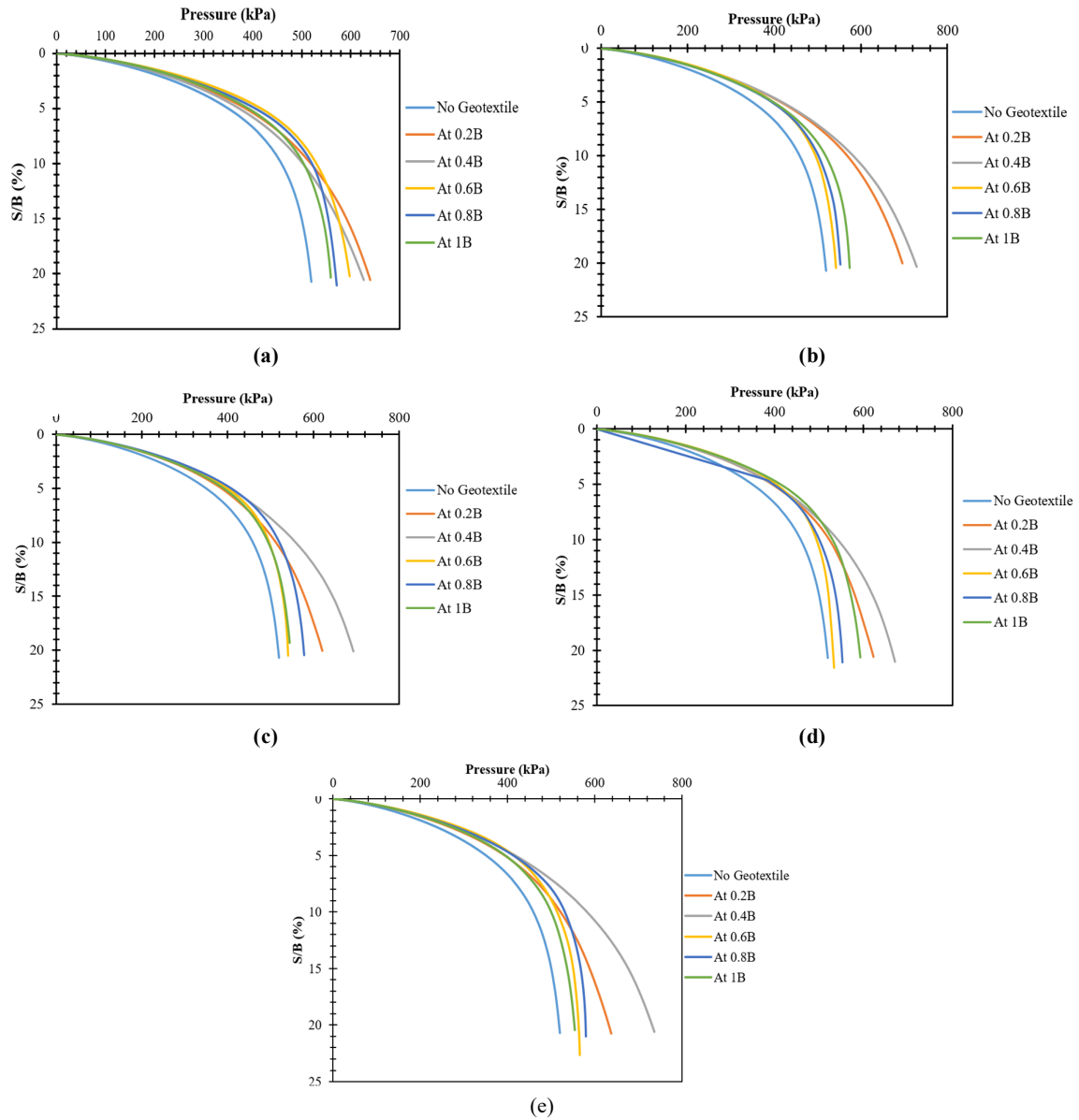


Figure 2. Pressure-Settlement Curves for soil at  $\phi=28^\circ$  (a)  $L = 1B$ , (b)  $L = 2B$ , (c)  $L = 3B$ , (d)  $L = 4B$ , and (e)  $L = 5B$ .

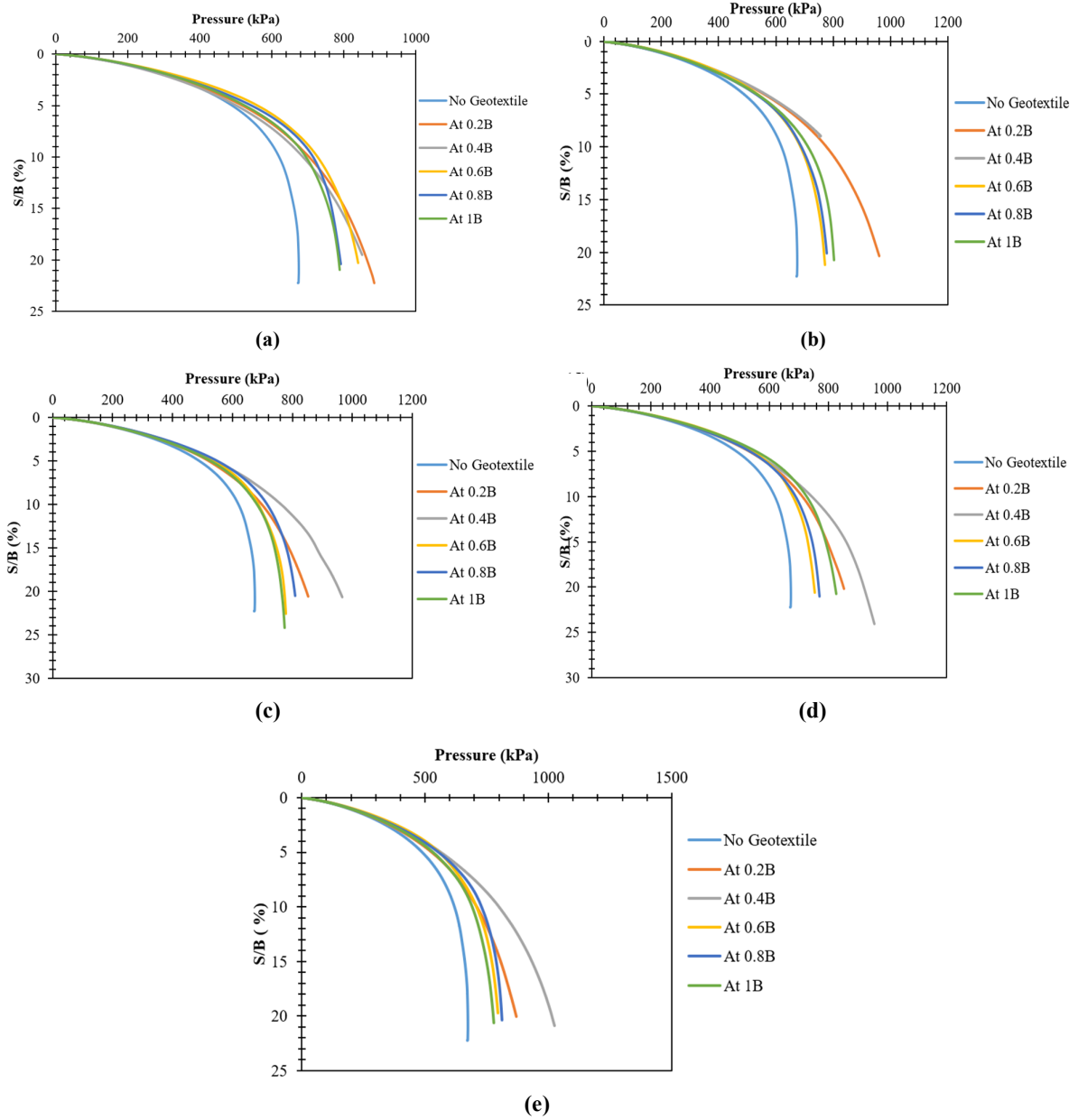


Figure 3. Pressure-Settlement Curves for soil at  $\phi = 30^\circ$  (a)  $L = 1B$ , (b)  $L = 2B$ , (c)  $L = 3B$ , (d)  $L = 4B$ , and (e)  $L = 5B$ .

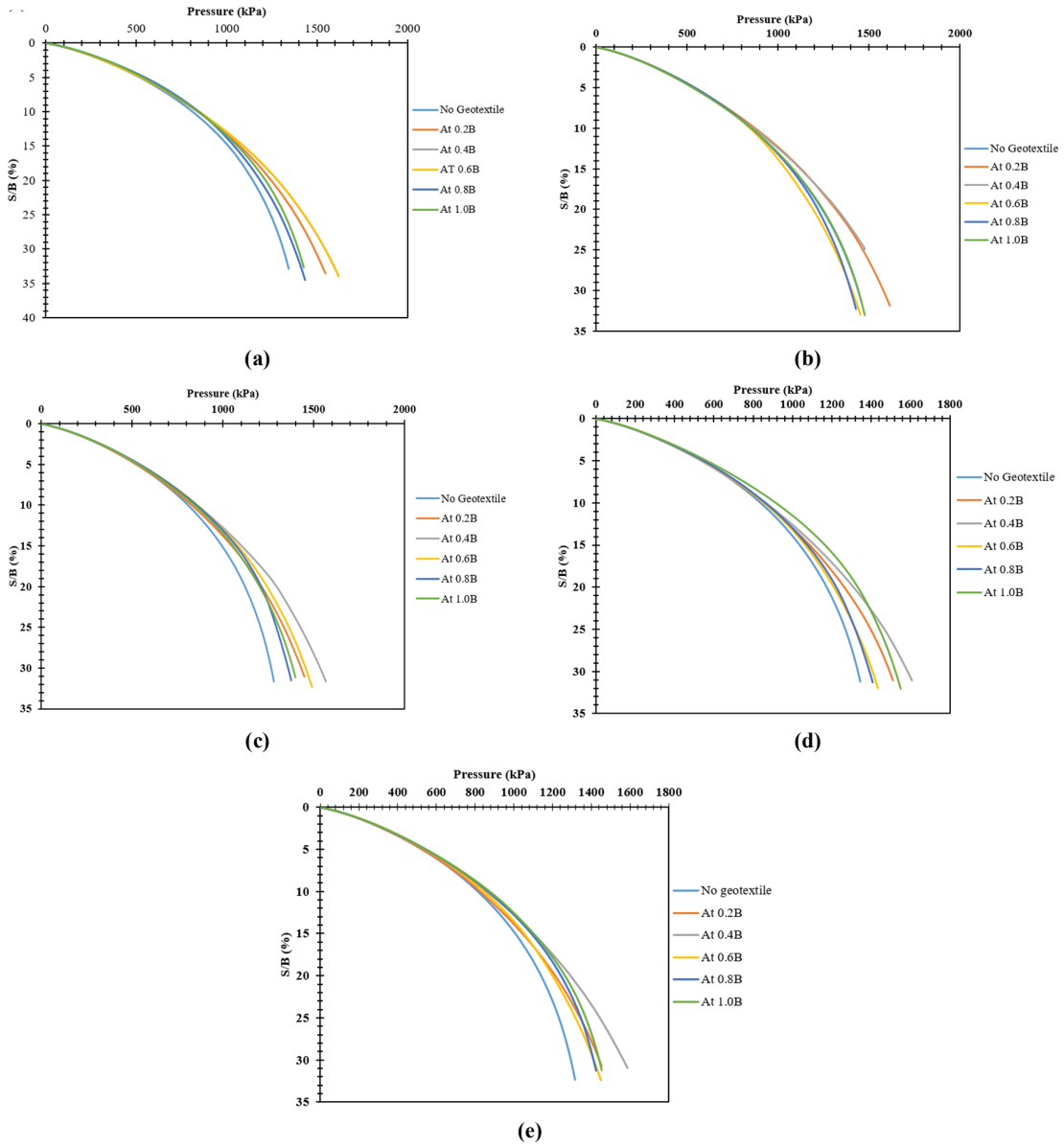


Figure 4. Pressure-Settlement Curves for soil at  $\phi = 34^\circ$  (a) L = 1B, (b) L = 2B, (c) L = 3B, (d) L = 4B, and (e) L = 5B.

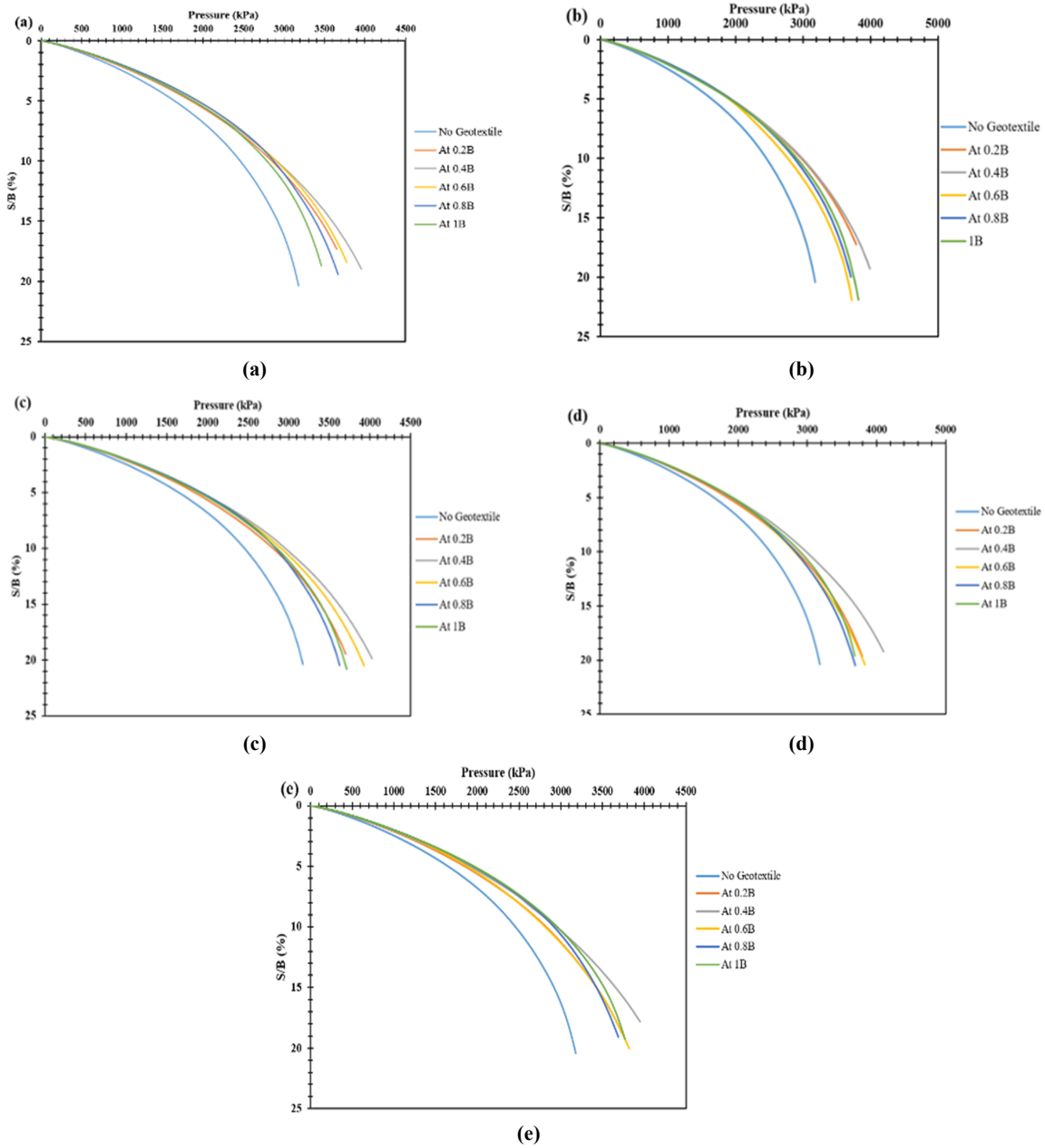


Figure 5. Pressure-Settlement Curves for soil at  $\phi = 38^\circ$  (a)  $L = 1B$ , (b)  $L = 2B$ , (c)  $L = 3B$ , (d)  $L = 4B$ , and (e)  $L = 5B$ .

### 3.1. Effect of depth of geotextile

Table 4 shows the ultimate bearing capacity of sand reinforced with coir geotextile for different values of  $\phi = 28^\circ$ ,  $\phi = 30^\circ$ ,  $\phi = 34^\circ$ , and  $\phi = 38^\circ$ , respectively. An increment in the ultimate bearing capacity of sand is observed after the application of the coir geotextile. The depth of geotextile placement plays a vital role in improvement in the bearing capacity of reinforced soil. For example, at length of the geotextile = 3B, the bearing capacity for soil at  $\phi = 30^\circ$  without geotextile was 619.78

kPa, and the bearing capacity for geotextile at different depths were 696.28 kPa, 761.79 kPa, 685.99 kPa, 715.16 kPa, 681.95 kPa for the depths at 0.2B, 0.4B, 0.6B, 0.8B, and 1B, respectively. The maximum improvement in bearing capacity was seen when coir geotextile was positioned at depth 0.4B from the base of footing. The presence of reinforcement prevents the lateral spreading of soil, thereby increasing the bearing capacity of soil. At depth of 0.4B, the coir geotextile may be more effective in transferring shear stresses and mobilizing the soil adjacent to the foundation. This

facilitates better interaction between the geotextile and the soil, potentially enhancing the bearing capacity. For the depths of 0.8B and 1B, the impact of coir geotextile on the increment of bearing

capacity was insignificant. It may be because when the coir geotextile is positioned deeper, its ability to distribute loads effectively may decrease, impacting the overall bearing capacity.

**Table 4. Result Variation of Bearing Capacity of soil with change in depth of coir geotextile.**

Angle of internal friction ( $\phi$ )	Length of the geotextile	Depth of the geotextile	Bearing Capacity (KPa)
28°	No geotextile	No geotextile	458.92
	1B	0.2B	518.412
	1B	0.4B	502.07
	1B	0.6B	529.70
	1B	0.8B	520.50
28°	1B	1.0B	503.37
	2B	0.2B	568.91
	2B	0.4B	583.23
	2B	0.6B	495.52
	2B	0.8B	501.54
28°	2B	1.0B	519.07
	3B	0.2B	512.83
	3B	0.4B	557.966
	3B	0.6B	525.46
	3B	0.8B	520.53
28°	3B	1.0B	494.89
	4B	0.2B	522.96
	4B	0.4B	541.99
	4B	0.6B	494.51
	4B	0.8B	500.93
28°	4B	1.0B	530.19
	5B	0.2B	521.22
	5B	0.4B	582.49
	5B	0.6B	514.22
	5B	0.8B	531.11
30°	5B	1.0B	499.93
	No geotextile	No geotextile	619.78
	1B	0.2B	703.66
	1B	0.4B	685.85
	1B	0.6B	727.17
30°	1B	0.8B	714.22
	1B	1.0B	695.133
	2B	0.2B	776.94
	2B	0.4B	752.26
	2B	0.6B	685.55
30°	2B	0.8B	689.55
	2B	1.0B	712.31
	3B	0.2B	696.28
	3B	0.4B	761.79
	3B	0.6B	685.99
30°	3B	0.8B	715.16
	3B	1.0B	681.95
	4B	0.2B	712.50
	4B	0.4B	744.40
	4B	0.6B	680.07
30°	4B	0.8B	689.58
	4B	1.0B	727.21
	5B	0.2B	709.82
	5B	0.4B	799.62
	5B	0.6B	709.27
30°	5B	0.8B	691.445
	5B	1.0B	728.88

**Continuous of Table 4. Result Variation of Bearing Capacity of soil with change in depth of coir geotextile.**

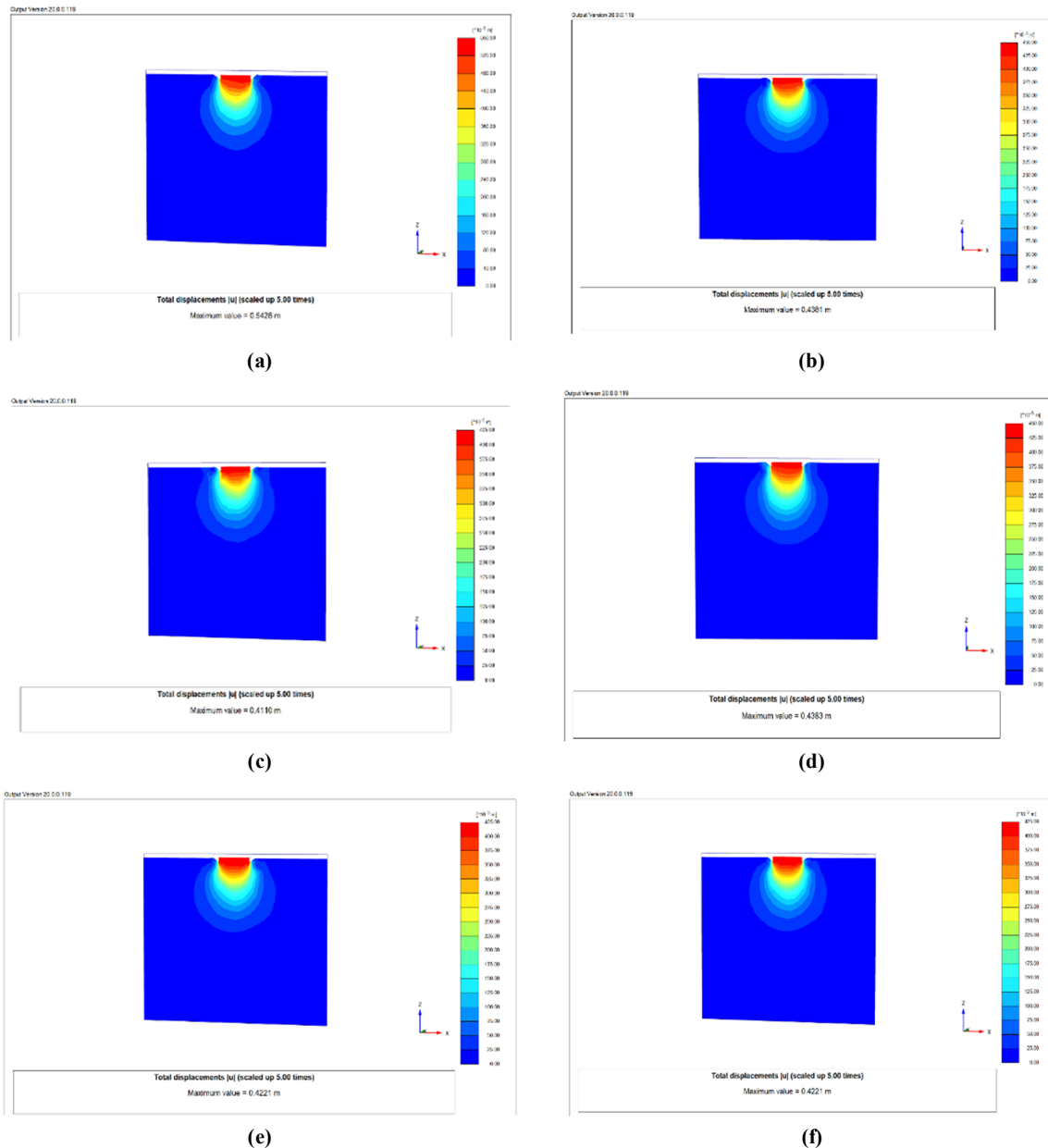
34°	No geotextile	No geotextile	809.88
	1B	0.2B	839.06
	1B	0.4B	847.90
	1B	0.6B	846.13
	1B	0.8B	855.07
34°	1B	1.0B	842.27
	2B	0.2B	873.98
	2B	0.4B	863.06
	2B	0.6B	846.16
	2B	0.8B	854.18
34°	2B	1.0B	853.13
	3B	0.2B	826.84
	3B	0.4B	857.62
	3B	0.6B	860.44
	3B	0.8B	855.35
34°	3B	1.0B	844.14
	4B	0.2B	855.12
	4B	0.4B	845.61
	4B	0.6B	855.00
	4B	0.8B	863.10
34°	4B	1.0B	916.79
	5B	0.2B	824.35
	5B	0.4B	860.46
	5B	0.6B	845.82
	5B	0.8B	868.72
38°	5B	1.0B	873.92
	No geotextile	No geotextile	2730.98
	1B	0.2B	2853.82
	1B	0.4B	2907.24
	1B	0.6B	2901.38
38°	1B	0.8B	2882.83
	1B	1.0B	2798.05
	2B	0.2B	2941.96
	2B	0.4B	2989.25
	2B	0.6B	2777.05
38°	2B	0.8B	2876.29
	2B	1.0B	2908.16
	3B	0.2B	2805.98
	3B	0.4B	2961.02
	3B	0.6B	2906.70
38°	3B	0.8B	2841.16
	3B	1.0B	2852.51
	4B	0.2B	2847.81
	4B	0.4B	2988.25
	4B	0.6B	2813.26
38°	4B	0.8B	2824.86
	4B	1.0B	2898.83
	5B	0.2B	2825.54
	5B	0.4B	2947.44
	5B	0.6B	2812.68
38°	5B	0.8B	2918.44
	5B	1.0B	2934.07

Figure 6 shows the total displacement of the soil sample with  $\phi = 34^\circ$ . It demonstrated that after applying coir geotextile, the total displacement of the sandy soil gets reduced. For example, the

maximum value of the displacement at  $\phi = 34^\circ$  without geotextile was 0.5428 m which was reduced to 0.4110 m after the application of coir geotextile at a depth of 0.4B. Hence, due to the

reinforcement action of coir geotextile with sand, a reduction of 24.3% was observed in the total

displacement when the geotextile layer was placed at 0.4B.



**Figure 6.** The displacement along the cross-section view for soil sample with  $\phi = 34^\circ$  (a) Soil sample without geotextile; (b) Geotextile is provided at 0.2B depth; (c) 0.4B depth; (d) 0.6B depth; (e) 0.8B depth; (f) 1.0B depth.

### 3.2. Effect of length of geotextile

From Figures 2 to 5, it can be concluded that by increasing the length of the geotextile from 1B to 5B, the total settlement of sand decreases. With the increment in the length of the coir geotextile, the ultimate bearing capacity rises over the increasing depth of the geotextile. A longer geotextile has a more widespread reinforcing effect inside the soil mass. A more thorough distribution of tensile stress

is made possible by this increased covering, which improves soil stability and decreases settlement. Additionally, a longer geotextile improves shear transfer mechanisms by providing a larger contact area between the geotextile and the soil. Better load-bearing capacity and less settlement are facilitated by this enhanced transmission of shear stresses into the soil matrix. The short anchorage length of coir geotextile layer is insufficient to mobilize lateral resistance created because of the

passive resistance, interlocking and friction compared to the transferred horizontal shear stresses.

**3.3. Effect of soil type on bearing capacity**

Bearing capacity ratio (BCR) is defined as the ratio of ultimate bearing capacity ( $Q_{ult}$ ) of square footing rested on coir geotextile reinforced sand to  $Q_{ult}$  of square footing rested on unreinforced sand. The formula for BCR is given in Equation (3):

$$BCR = \frac{UBC \text{ of reinforced sand}}{UBC \text{ of unreinforced sand}} \quad (3)$$

Figures 7(a)–(d) illustrate the variation of BCR with  $d/B$  ratio for various values angles of internal friction  $\phi = 28^\circ$ ,  $\phi = 30^\circ$ ,  $\phi = 34^\circ$ , and  $\phi = 38^\circ$ , respectively. From Figures 7(a)-(d), it can be concluded that with the increase of the angle of internal friction of the sand at the certain level; the

BCR first increases then decreases for the higher angles of internal friction. The BCR increases for sands with  $\phi = 28^\circ$  and  $\phi = 30^\circ$ , whereas it decreases for sand  $\phi = 34^\circ$  and  $\phi = 38^\circ$ . This decrease in the BCR of sand reinforced with coir geotextile observed at higher values of  $\phi$  may be due the interlock between the individual particles of sand is more effective at higher angles of internal friction. Nevertheless, the interlocking process may be hampered by the presence of coir geotextile, lowering the direct particle-to-particle contact. At lower values of angles of internal friction, the coir geotextile gives the reinforced sand more tensile strength. With larger angles of internal friction, the sand's cohesionless nature becomes more important, and the relative increase from the geotextile may decrease. Hence, the coir geotextile gives maximum improvement in the BCR for  $\phi = 30^\circ$ .

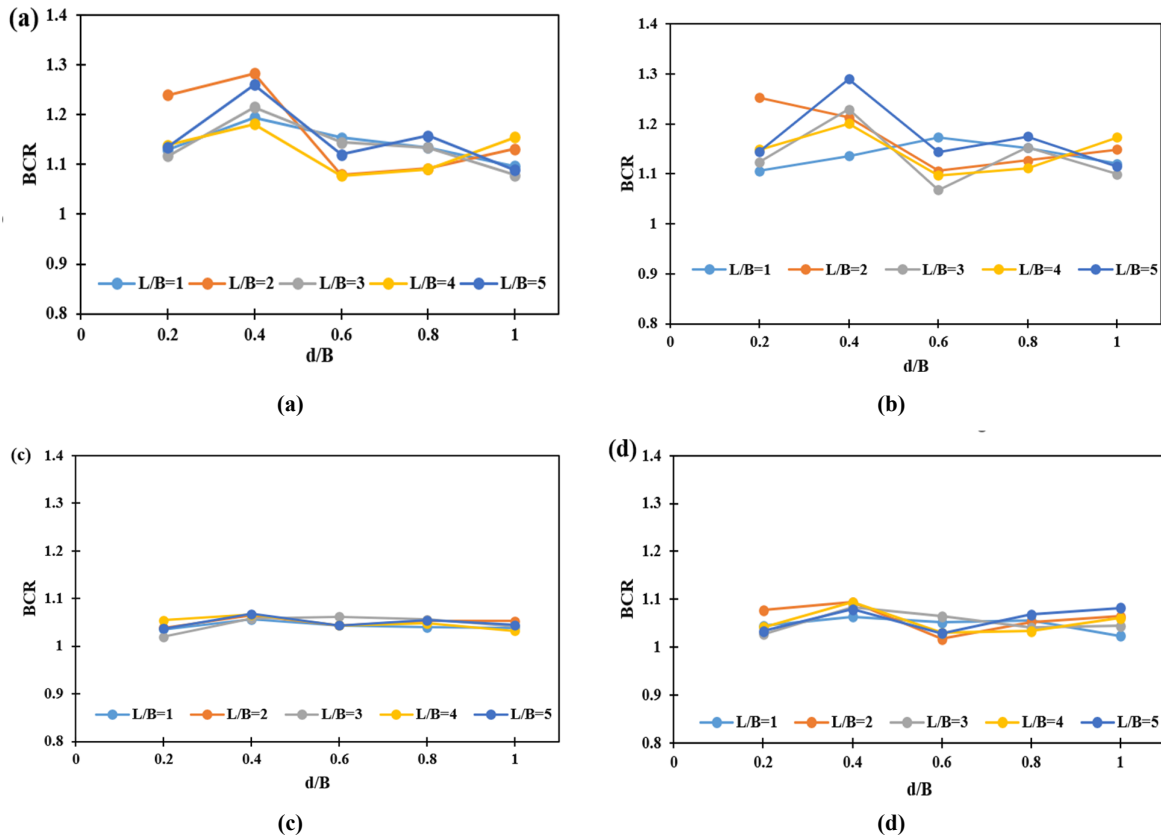


**Figure 7. Bearing capacity ratio (BCR) curves obtained for various angle of friction (a)  $\phi=28^\circ$ , (b)  $\phi = 30^\circ$ , (c)  $\phi = 34^\circ$ , and (d)  $\phi = 38^\circ$ .**

**4. Regression Analysis**

Regression analysis is described as one of the statistical techniques used for determining a connection between the set of dependent and independent variables [47,48]. Furthermore, the

regression analysis determines the coefficients, which cause the function to best fit with the detected data that is shown. With the aim of enumerating particular parameters, for example angle of internal friction, length, and depth of the

geotextile, each model test outcome was examined with the application of the SPSS program V.28. Also, the linear regression model is specified for explaining the foundation behaviors.

In this analysis, the ultimate bearing capacity of coir geotextile-reinforced sandy soil was stated as a dependent variable regarding to regression analysis. Moreover, the influencing parameters, comprising the angle of internal friction, length of the geotextile, and depth of the geotextile specified as independent variables. Equation (4) showed the expression developed for the ultimate bearing capacity of coir geotextile-treated sand foundations:

$$Q_{ult} = 6.159L + 2.108D + 219.785\phi - 5921.805 \quad (4)$$

where  $Q_{ult}$  is the ultimate bearing capacity of the sandy soil,  $L$  is the length of the geotextile,  $D$  is the

depth at which the geotextile is placed, and  $\phi$  is the angle of internal friction. The coefficient of determination ( $R^2$ ) was found to be 0.77, which shows that data is closely fitted to the regression equation.

Figure 8 shows the deviation of numerical and predicted ultimate bearing capacity for square footing rested on sand treated with coir geotextile. From the equation features, the correlation of inputs (the angle of internal friction, length of the geotextile, and depth of the geotextile) with the ultimate bearing capacity of the soil can be observed. It is noted that  $Q_{ult}$  of the sandy soil is highly correlated to the angle of internal friction, followed by the length and depth of the geotextile, where it affects the direct relationship.

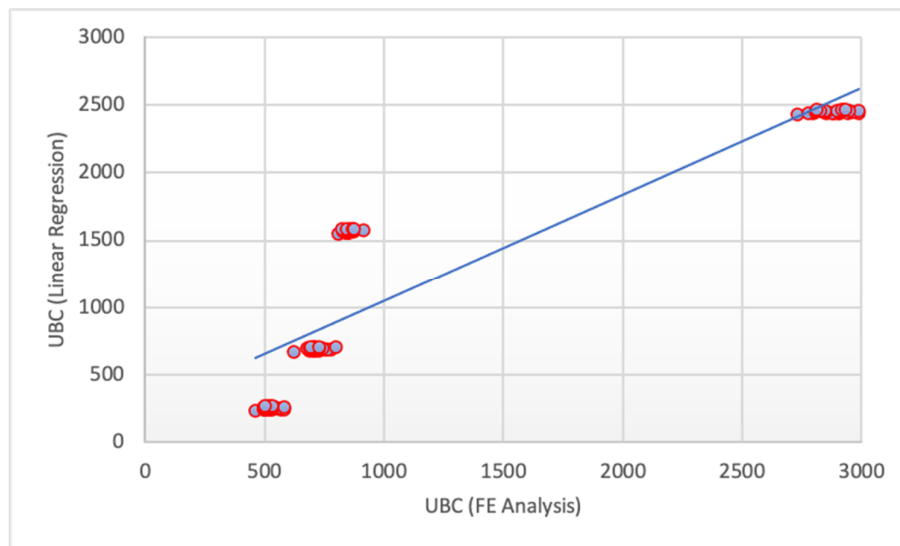


**Figure 8. Variation of numerical and predicted ultimate bearing capacity for square footing rested on sand reinforced with coir geotextile.**

Basically, the regression analysis to generalize the results associated to the models was not tremendously justified; however, there is an ability for indicating the importance regarding each of the studied parameters.

## 5. Conclusions

The following conclusions can be drawn from this study:

1. The bearing capacity of sand increases by placing coir geotextiles up to a depth of  $0.4B$ . Hence, the optimal depth for placement of geotextile was obtained as at  $0.4B$ .
2. A total increase of 29% in bearing capacity of sand and a total reduction of 24.3% in total

displacement was observed when the geotextile was placed at the optimum depth, compared to the unreinforced sand.

3. It was observed that the bearing capacity of sand increases with the increase in length of geotextile. Hence, from the BCR curves, the optimum length of coir geotextile was found as  $4B$ - $5B$ .
4. An insignificant improvement in the bearing capacity ratio of sand reinforced with coir geotextile was observed at higher values of angle of internal friction.
5. The maximum increase in the BCR was for  $\phi = 30^\circ$ ,  $L = 5B$ , and  $D = 0.4B$ .

## References:

- [1]. Shekhawat, P., Sharma, G., & Singh, R.M. (2023). Strength characteristics of hazardous wastes flyash and eggshell powder-based geopolymer-stabilized soft soil cured at ambient temperature. *Arabian Journal of Geoscience*, 16, 1–12.
- [2]. Terzaghi, K. (1943). *Theoretical Soil Mechanics*, John Wiley & Sons, New York.
- [3]. Meyerhof, G.G. (1951). The ultimate bearing capacity of foundations. *Geotechnique*, 2, 301–332.
- [4]. Hansen, J.B. (1961). A General Formula for Bearing Capacity. *Danish Geotech Institute, Copenhagen, Bulletin 1*.
- [5]. Vesić, A.S. (1973). Discussion of “Bearing Capacity Theory from Experimental Results.” *Journal of the Soil Mechanics and Foundations Division*, 99, 575–577.
- [6]. Sridhar, R., & Prathap Kumar, M.T. (2017). Behaviour of model footing resting on sand reinforced with number of layers of coir geotextile. *Innovative Infrastructure Solution*, 2, 1–8. <https://doi.org/10.1007/s41062-017-0099-y>.
- [7]. Akhil, K.S., Sankar, N., & Chandrakaran, S. (2019). Behaviour of model footing on bamboo mat-reinforced sand beds. *Soils and Foundations*, 59, 1324–1335.
- [8]. Sharma, A., & Singh, K. (2020). Bearing Capacity of Sand Admixed Pond Ash Reinforced with Natural Fiber. *Journal of Natural Fibers*, 00, 1–14.
- [9]. Kolathayar, S., Sowmya, S. & Priyanka, E. (2020). Comparative Study for Performance of Soil Bed Reinforced with Jute and Sisal Geocells as Alternatives to HDPE Geocells. *International Journal of Geosynthetics and Ground Engineering*, 6, 1–8.
- [10]. Sharma, A., & Nallasivam, K. (2023). Comparison of Bearing Capacity Behavior of Strip Footing Resting on Sand-Admixed Pond Ash Reinforced with Natural Fiber and Geogrid. *Indian Geotechnical Journal*, 1-18.
- [11]. Yaylaci, M., Abanoz, M., Yaylaci, E.U., Olmez, H., Sekban, D.M., & Birinci A. (2022). The contact problem of the functionally graded layer resting on rigid foundation pressed via rigid punch. *Steel and Composite Structures*, 43, 661.
- [12]. Yaylaci, M., Yayli, M., Yaylaci, E.U., Olmez, H., & Birinci, A. (2021). Analyzing the contact problem of a functionally graded layer resting on an elastic half plane with theory of elasticity, finite element method and multilayer perceptron. *Structural Engineering and Mechanics*, 78, 585–97.
- [13]. Yaylaci, M., Yaylaci, E.U., Özdemir, M.E., Öztürk, Ş., & Sesli, H. (2023). Vibration and buckling analyses of FGM beam with edge crack: Finite element and multilayer perceptron methods. *Steel and Composite Structures*, 46(4), 565.
- [14]. Özdemir, M.E., & Yaylaci, M. (2023). Research of the impact of material and flow properties on fluid-structure interaction in cage systems. *Wind and structures*, 36, 31.
- [15]. Adıyaman, G., Öner, E., Yaylaci, M., & Birinci, A. (2023). A study on the contact problem of a layer consisting of functionally graded material (FGM) in the presence of body force. *Journal of Mechanics of Materials and Structures*, 18, 125–141.
- [16]. Shekhawat, P., Shrivastava, S., & Shrivastava, N. (2019). Agricultural Waste Utilization in Sustainable and Resilient Construction. *Springer Singapore*.
- [17]. Tan, T., Huat, B.B.K., Anggraini, V., & Shukla, S.K. (2021). Improving the engineering behaviour of residual soil with fly ash and treated natural fibres in alkaline condition. *International Journal of Geotechnical Engineering*, 15, 313–326.
- [18]. Tan T., Huat, B.B.K., Anggraini, V., Shukla, S.K., & Nahazanan, H. (2021). Strength Behavior of Fly Ash-Stabilized Soil Reinforced with Coir Fibers in Alkaline Environment. *Journal of Natural Fibers*, 18, 1556–1569.
- [19]. Yadav, J.S., & Tiwari, S.K. (2016). Behaviour of cement stabilized treated coir fibre-reinforced clay-pond ash mixtures. *Journal of Building Engineering*, 8, 131–140.
- [20]. Yadav, J.S., Tiwari, S.K., & Shekhwat, P. (2018). Strength Behaviour of Clayey Soil Mixed with Pond Ash, Cement and Randomly Distributed Fibres. *Transportation Infrastructure Geotechnology*, 5.
- [21]. Kamaruddin, F.A., Nahazanan, H., Huat, B.K., & Anggraini, V. (2020). Improvement of marine clay soil using lime and alkaline activation stabilized with inclusion of treated coir fibre. *Applied Sciences (Switzerland)*, 10.
- [22]. Kamaruddin, F.A., Anggraini, V., Huat, B.K., & Nahazanan, H. (2020). Wetting/drying behavior of lime and alkaline activation stabilized marine clay reinforced with modified coir fiber. *Materials (Basel)*, 13, 1–18.
- [23]. Kar, R.K., Pradhan, P.K., & Naik, A. (2014). Effect of randomly distributed coir fibers on strength characteristics of cohesive soil. *Electronic Journal of Geotechnical Engineering*, 19 G, 1567–83.
- [24]. Menezes, L.C.P., Sousa, D.B., Sukar, S.F., & Ferreira, S.R.M. (2019). Analysis of the Physical-Mechanical Behavior of Clayey Sand Soil Improved with Coir Fiber. *Soils and Rocks*, 42, 31–42.
- [25]. Sivakumar Babu, G.L., Vasudevan, A.K., Vinod, P., & Ajitha, B. (2009). Discussion: Evaluation of strength and stiffness response of coir-fibre-reinforced soil. *Proceedings of the Institution of Civil Engineers: Ground Improvement*, 162, 205–207.
- [26]. Mittal, A. (2021). Effect of coir fibres on strength, thickness and cost of PMGSY roads. *IOP Conference*

Series: *Materials Science and Engineering*, 1136, 012042.

[27]. Khatri, V.N., Dutta, R.K., & Katre, S. (2017). Shear strength, bearing ratio and settlement behavior of clay reinforced with chemically treated coir fibres. *Jordan Journal of Civil Engineering*, 11, 659–679.

[28]. Singh, H., & Hussain, Y. (2020). Utilization of waste coir fiber with polypropylene fiber for soil stabilization. *Journal of Green Engineering*, 10, 6076–6089.

[29]. Widiyanti, A., Diana, W., & Alghifari, M.R. (2021). Shear Strength and Elastic Modulus Behavior of Coconut Fiber-Reinforced Expansive Soil. *IOP Conference Series: Materials Science and Engineering*, 1144, 012043.

[30]. Rao, G.V., Dutta, R.K., & Ujwala, D. (2005). Strength characteristics of sand reinforced with coir fibres and coir geotextiles. *Electronic Journal of Geotechnical Engineering*, 10 G.

[31]. Sayida, M.K., Evangeline, S.Y., & Girish, M.S. (2020). Coir Geotextiles for Paved Roads: A Laboratory and Field Study Using Non-Plastic Soil as Subgrade. *Journal of Natural Fibers*, 17, 1329–1344.

[32]. Lal, D., Sankar, N., & Chandrakaran, S. (2017). Performance of Shallow Foundations Resting on Coir Geotextile Reinforced Sand Bed. *Soil Mechanics and Foundation Engineering*, 54, 60–64.

[33]. Lal, D., Sankar, N., & Chandrakaran, S. (2017). Effect of reinforcement form on the behaviour of coir geotextile reinforced sand beds. *Soils and Foundations*, 57, 227–236.

[34]. Lal, D., Sankar, N., & Chandrakaran S. (2018). Effect of reinforcement form on the behaviour of coir geotextile-reinforced sand through laboratory triaxial compression tests. *International Journal of Geotechnical Engineering*, 12, 309–315.

[35]. Vinod, P., & Bhaskar, A.B. (2012). Model studies on woven coir geotextile-reinforced sand bed. *Proceedings of the Institution of Civil Engineers: Ground Improvement*, 165, 53–57.

[36]. Subaida, E.A., Chandrakaran, S., & Sankar N. (2008). Experimental investigations on tensile and pullout behaviour of woven coir geotextiles. *Geotextiles and Geomembranes*, 26, 384–392.

[37]. Entidhar, T. Al-Taie. (2019). Evaluation of Settlement and Bearing Capacity of Embankment on Soft Soil With Reinforced Geogrids. *International Journal of Engineering Research and Technology*, V8.

[38]. Al-Ameri, A.F., Hussein, S.A., & Mekkiyah, H.

(2020). Estimate the bearing capacity of full-scale model shallow foundations on layered-soil using PLAXIS. *Solid State Technology*, 63, 1775–1787.

[39]. Yaylaci, M., Abanoz, M., Yaylaci, E.U., Ölmez, H., Sekban, D.M., & Birinci, A. (2022). Evaluation of the contact problem of functionally graded layer resting on rigid foundation pressed via rigid punch by analytical and numerical (FEM and MLP) methods. *Archive of Applied Mechanics*, 92, 1953–1971.

[40]. Turan, M., Uzun, Yaylaci, E., & Yaylaci, M. (2023). Free vibration and buckling of functionally graded porous beams using analytical, finite element, and artificial neural network methods. *Archive of Applied Mechanics*, 93, 1351–1372.

[41]. Yaylaci, M., Şabano, B.Ş., Özdemir, M.E., & Birinci, A. (2022). Solving the contact problem of functionally graded layers resting on a HP and pressed with a uniformly distributed load by analytical and numerical methods. *Structural Engineering and Mechanics, An Int'l Journal*, 82, 401–416.

[42]. Yaylaci, E.U., Öner, E., Yaylaci, M., Özdemir, M.E., Abushattal, A., & Birinci, A. (2022). Application of artificial neural networks in the analysis of the continuous contact problem. *Structural Engineering and Mechanics, An Int'l Journal*, 84, 35–48.

[43]. Yaylaci, M. (2022). Simulate of edge and an internal crack problem and estimation of stress intensity factor through finite element method. *Advances in nano research*, 12, 405.

[44]. Yaylaci, M., Uzun Yaylaci, E., Özdemir, M.E., Ay, S., & Öztürk, S. (2022). Implementation of finite element and artificial neural network methods to analyze the contact problem of a functionally graded layer containing crack.

[45]. Yaylaci, M. (2016). The investigation crack problem through numerical analysis. *Structural Engineering and Mechanics, An Int'l Journal*, 57, 1143–1156.

[46]. Öner, E., Şengül Şabano, B., Uzun Yaylaci, E., Adiyaman, G., Yaylaci, M., & Birinci A. (2022). On the plane receding contact between two functionally graded layers using computational, finite element and artificial neural network methods. *ZAMM-Journal of Applied Mathematics and Mechanics/Zeitschrift für Angewandte Mathematik und Mechanik*, 102, e202100287.

[47]. Devore, J.L., & Farnum, N.R. (1999). Statistics for engineers and scientists.

[48]. Dielman, T.E. (2001). Applied regression analysis for business and economics. *Duxbury/Thomson Learning Pacific Grove, CA*.

## ارزیابی پاسخ ته نشینی فشار پایه مربعی تکیه بر شن و ماسه تقویت شده با ژئوتکستایل کویر

جیتندرا سینگ یاداو<sup>۱</sup>، پونام شخوات<sup>۲\*</sup>، و اسریک‌شاوا کی سی<sup>۲</sup>

۱. گروه مهندسی عمران، NIT Kurukshetra، هند

۲. گروه مهندسی عمران، موسسه فناوری جیوتی، پنگلور، هند

ارسال ۲۰۲۳/۱۰/۱۳، پذیرش ۲۰۲۳/۱۲/۲۱

\* نویسنده مسئول مکاتبات: poonam.s@jyothyit.ac.in

## چکیده:

هدف کار حاضر ارزیابی رفتار ته نشینی فشار بسترهای شن و ماسه در زیر یک پایه مربع تقویت شده با ژئوتکستایل کویر با استفاده از نرم افزار PLAXIS 3D است. زاویه اصطکاک داخلی ماسه از ۲۸ درجه تا ۳۸ درجه متغیر بود. تأثیر طول ژئوتکستایل زغال سنگ (1B، 2B، 3B، 4B، و 5B؛ B عرض پایه است) و موقعیت ژئوتکستایل زغالی (0.2B، 0.4B، 0.6B، 0.8B، و 1B) بر ظرفیت باربری نهایی شن و ماسه مورد بررسی قرار گرفت. بهبود قابل توجهی در ظرفیت باربری نهایی بسترهای شنی با تهیه ژئوتکستایل های زغالی حاصل شد. مشاهده شد که ظرفیت باربری شن و ماسه با قرار دادن ژئوتکستایل های زغالی تا عمق 0.4B از پایه پایه افزایش می یابد و پس از آن شروع به کاهش می کند. طول بهینه ژئوتکستایل کویر 4B-5B یافت شد. بهبود ناچیز در نسبت ظرفیت باربری شن و ماسه تقویت شده با ژئوتکستایل کویر در مقادیر بالاتر زاویه اصطکاک داخلی مشاهده شد.

**کلمات کلیدی:** ژئوتکستایل کویر، ظرفیت باربری نهایی، شن و ماسه، مدل سازی عددی.